Pergamon

Bioorganic & Medicinal Chemistry 8 (2000) 413–426

BIOORGANIC & MEDICINAL CHEMISTRY

An Investigation of Antibody Acyl Hydrolysis Catalysis Using a Large Set of Related Haptens

Amy L. Odenbaugh, Eric D. Helms and Brent L. Iverson*

The Department of Chemistry and Biochemistry, The University of Texas at Austin, Austin, TX 78712, USA

Received 16 July 1999; accepted 8 November 1999

Abstract—An aspect of catalytic antibody research that receives little attention in the literature involves hapten systems that fail to elicit antibody catalysts despite a high affinity immune response and hapten designs that resemble those known to elicit catalysts. We have investigated a series of 12 phosphate and phosphonate haptens in a total of three animal systems. Dramatic and reproducible differences were observed in the catalytic activities of polyclonal antibodies elicited by the different haptens. A phosphate hapten with a phenyl ring on the side of the hapten opposite the linker elicited reproducibly high levels of polyclonal antibody catalytic activity. The other 11 haptens, most with benzyl groups on the side of the hapten opposite the linker, elicited immune responses in which catalytic activity was significantly weaker in terms of the level of observed catalytic activity, as well as frequency of elicited catalysts. Our results indicate that subtle features of transition state analogue hapten structure can have a dramatic and reproducible influence over the catalytic activity of elicited antibodies in related haptens. Whatever the explanation, subtle changes in mechanistic features due to altered leaving group ability/location or overall hapten flexibility, the comprehensive data presented here indicate that phenyl or 4-nitrophenyl leaving groups located opposite the hapten linker are to be preferred in order to elicit highly active antibody catalysts for acyl hydrolysis reactions.

Introduction

An aspect of catalytic antibody research that receives little attention in the literature involves those hapten systems that fail to elicit antibody catalysts despite a high affinity immune response and hapten designs that resemble those known to elicit catalysts. A better understanding of hapten structural features that lead to a reduced or complete lack of elicited catalytic activity would dramatically aid in the design of future haptens.

At least two conditions must theoretically be met for a transition state analogue hapten to elicit antibody catalytic activity by design. First, it is assumed to be necessary, but not sufficient, that the transition state analogue has some structural features in common with the rate-limiting transition state, such as charge distribution and geometry, that are not found in starting material(s) or product(s). Second, it is also assumed that the binding energy within elicited antibody binding pockets is partitioned in such a way that substrate binds, then is facilitated along the *entire* reaction path. Failure to meet this second condition, either by failing to allow substrate binding or by binding substrate in such a way that catalytic product formation is not favored, is presumably the reason so many high affinity antibodies elicited by transition state analogue haptens fail to affect catalysis of a desired reaction with substrate. Gaining a predictive understanding of how overall hapten structure affects this second condition will require an understanding of how different structural features of a hapten are recognized by elicited antibodies.

The advent of polyclonal catalytic antibody studies involving immunization with a transition state analogue hapten makes possible the *systematic* study of hapten structure in the context of elicited antibody recognition

Keywords: polyclonal catalytic antibodies; acyl hydrolysis.

Abbreviations: k_{cat}, catalytic rate constant, calculated as $V_{max}/2$[IgG] where [IgG] is measured through quantitative inhibition experiments with hapten while V_{max} and K_M are the maximum catalytic velocity and Michaelis constant, respectively, derived from the Lineweaver–Burk analysis; k_{uncat}, rate of reaction in the absence of added catalyst; KLH, keyhole limpet hemocyanin; BSA, bovine serum albumin; ELISA, enzyme-linked immunosorbent assay; PBS, phosphate buffered saline; EDC, [1-ethyl-3-(dimethylamino)propyl]carbodiimide; DMF, *N,N*-dimethylformamide; THF, tetrahydrofuran; MS, mass spectral analysis; FAB, fast atom bombardment; DCC, dicyclohexylcarbodiimide; HOBt, 4-hydroxybenzotriazole; K_A, equilibrium association constant; K_D, equilibrium dissociation constant calculated as $1/K_A$; nm, not measured; nd, none detected; Tris, tris(hydroxymethyl)aminomethane.

*Corresponding author. Tel.: +1-512-471-5053; fax: +1-512-417-8696.

0968-0896/00/$ - see front matter
PII: S0968-0896(99)00302-8

and catalytic activity for an entire immune response.[1–21] For example, a systematic study from our laboratory involving the replacement of a single atom in a transition state analogue hapten–substrate system found that optimum catalysis was observed when the hapten and substrate were most similar in structure.[12] A different study uncovered a striking relationship between hapten size/hydrophobicity and catalysis.[13] Specifically, a series of phosphate haptens with large aromatic substituents elicited antibodies that were not catalytic, but bound strongly to the aromatic portions of their haptens and substrates. Similar phosphate haptens with smaller aromatic groups elicited antibodies with catalytic activity that was inversely correlated to the size of the aromatic group. This latter study has verified by systematic experiment that the level of elicited catalytic activity can be modulated in dramatic fashion by structural features *distinct* from the portion of the hapten intended to mimic uniquely a rate-limiting transition state.

The present study involves a series of 12 phosphate and phosphonate haptens, all of which have structural features that should have made them capable of eliciting active polyclonal catalytic antibodies. We found that six haptens, in the form of three pairs of enantiomers, failed to induce any catalytic activity in rabbit polyclonal antibodies despite the presence of high affinity and highly specific immune responses. This surprising result led to the investigation of a series of benzyl phosphate haptens in three different animal models. For the entire series of haptens, the elicited catalytic activity was significantly weaker in terms of the level of observed catalytic activity, as well as frequency of elicited catalysts, compared to a phenyl phosphate hapten we have used previously. In summary, our results indicate that only a hapten with a phenyl group on the side of the hapten opposite the linker was able to elicit reproducibly high levels of polyclonal catalytic activity. Taken with mechanistic investigations also described, our findings suggest that increased flexibility and/or extremely subtle mechanistic differences may be operating to limit significantly elicited catalytic activity.

Results

The six (three enantiomeric pairs) phosphonate and phosphate haptens **1**–**6** shown in Scheme 1 were synthesized and coupled to keyhole limpet hemocyanin (KLH). These haptens were designed to elicit catalysts for the $B_{AC}2$ hydrolysis of the corresponding ester and carbonate substrates **8**–**13**. The hapten–KLH conjugates were used to immunize New Zealand white rabbits five times at 21-day intervals using standard protocols. In *each* case, no catalysis of the corresponding substrates was observed in the elicited polyclonal response in any of the serum samples that were removed 10 days following both the third and fifth immunizations. Importantly, as indicated by the relative dissociation constants determined after the fifth immunization for each sample and listed in Table 1, high affinity antibodies were elicited by these immunizations. These relative dissociation constants were determined using competition ELISA, a technique that accurately ranks relative affinities, although the absolute affinities may be underestimated.[22–24] As expected, each sample retained the ability to discriminate between enantiomers, and the immunizing hapten was always substantially preferred relative to its enantiomer. Substrate binding in the range of 1×10^2 to 8×10^3 M^{-1} was observed for the antibodies elicited against haptens **5** and **6** by competition ELISA, but limited polyclonal sample precluded the measurement of substrate binding for the antibodies raised against haptens **1**–**4**.

A positive control experiment was carried out using the rabbit originally immunized with hapten **3** and the rabbit originally immunized with hapten **4**. Six months

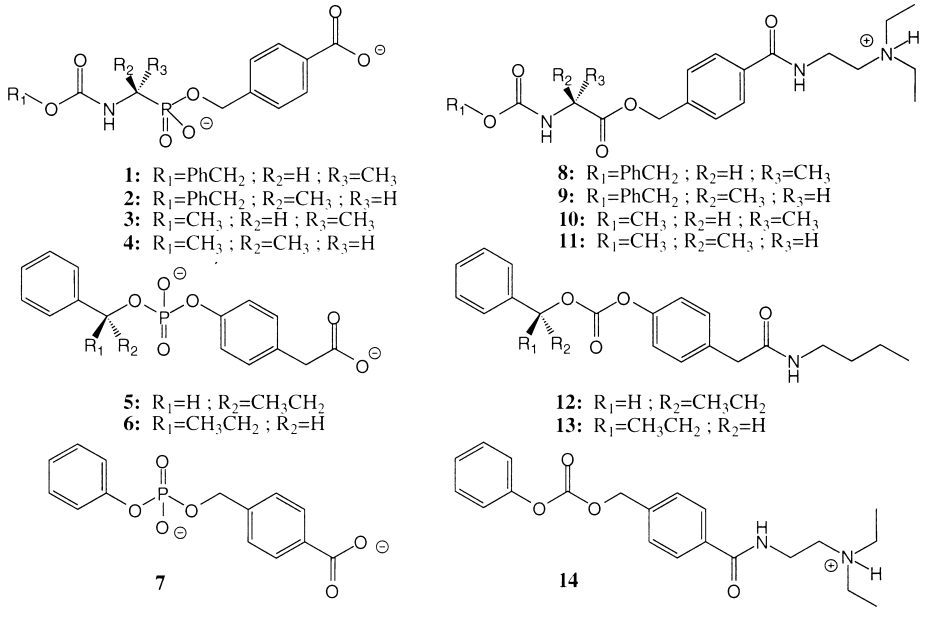

Scheme 1. Structures of haptens **1**–**7** and substrates **8**–**14**.

Table 1. Apparent dissociation constants, K_D (μM), for the indicated haptens and substrates measured for the various samples of New Zealand white rabbit polyclonal antibodies as determined by competition ELISA[a]

Rabbit #/antibodies	Hapten	K_D (μM)	Substrate	K_D (μM)
2403/anti-**1**	**1**	< 0.1 (±0.4)		
	2	20 (±2)		
2401/anti-**2**	**2**	0.6 (±0.2)		
	1	80 (±9)		
2509/anti-**3**	**3**	0.7 (±0.3)		
	4	70 (±10)		
2510/anti-**4**	**4**	0.4 (±0.1)		
	3	50 (±6)		
2164/anti-**5**	**5**	10 (±2)	**12**	8000
	6	800 (±80)		
2165/anti-**5**	**5**	80 (±10)	**12**	1000
	6	600 (±60)		
2162/anti-**6**	**6**	100 (±10)	**13**	200
	5	3000 (±700)		
2163/anti-**6**	**6**	0.2 (±0.9)	**13**	27
	5	300 (±50)		

[a]Standard deviations of repetitive ELISA measurements are shown in parentheses.

following the last immunization with either **3** or **4**, each rabbit was immunized five times at 21-day intervals with the phenyl phosphate hapten **7**. Polyclonal antibodies isolated from the sera of both rabbits 10 days following the fifth immunization displayed considerable catalytic activity with the carbonate substrate **14**. Lineweaver–Burk analyses were used to determine apparent K_M and V_{max} values.[4] These values are termed 'apparent' to emphasize that they characterize the polyclonal samples as a whole rather than any one catalytic antibody species. The fraction of high affinity, hapten-specific antibodies were measured for each sample by carrying out quantitative inhibition studies with hapten.[4] These fractions were used to estimate catalyst concentration in order to calculate the values of apparent k_{cat} and apparent k_{cat}/k_{uncat} that are listed in Table 2.

The *para*-substituted benzyl haptens **15**–**19** were prepared and coupled to KLH (Scheme 2). These haptens were designed to elicit catalysts for the hydrolysis of the correspondingly substituted benzyl carbonate substrates **20**–**24**. Each hapten–KLH conjugate was used to immunize a different set of 10 BALB/cJ mice a total of five times at 21-day intervals. As a control, polyclonal antibodies were also elicited from a separate set of 10 BALB/cJ mice using underivatized KLH. Serum was removed 10 days after the fifth immunization from each of the ten animals immunized with the same hapten. The 10 serum samples were combined and the polyclonal antibodies isolated from the pooled sera. Pooling

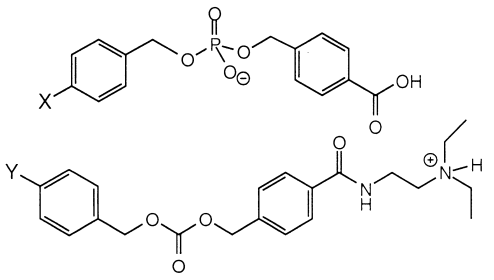

15: X = NO_2 **20:** Y = NO_2
16: X = Cl **21:** Y = Cl
17: X = H **22:** Y = H
18: X = OMe **23:** Y = OMe
19: X = OEt **24:** Y = OEt

Scheme 2. Structures of haptens **15**–**19** and substrates **20**–**24**.

of the sera is required for catalytic polyclonal antibody studies carried out in mice because of the small volume of serum present in a single mouse. Pooling of sera also reduces experimental artifacts derived from differences in the immune responses of individual animals.

For the polyclonal antibody samples that were catalytic for hydrolysis of their most homologous substrates, apparent K_M, V_{max} and k_{cat}/k_{uncat} were determined (Table 3). Overall, the samples elicited by **15**–**17** displayed similar levels of catalytic activity, with apparent k_{cat}/k_{uncat} values ranging from 420 to 1250.

While the anti-**18** and anti-**19** samples were not catalytic for hydrolysis of their most homologous substrate, these samples were capable of catalyzing the hydrolysis of substrates **20**–**22**. This unusual substrate specificity likely results from a change in mechanism for substrates **23** and **24**, so that the haptens **18** and **19** no longer resemble a rate-limiting transition state for cleavage. The pH dependence of hydrolysis of all the benzyl carbonate substrates was investigated in the absence of any polyclonal antibody catalysts. Carbonates **20**–**22** hydrolyzed in a base-dependent fashion, as expected for the $B_{AC}2$ mechanism. Substrates **23** and **24** hydrolyzed in a pH *independent* fashion, indicating that these substrates hydrolyze by a mechanism different from $B_{AC}2$. Although more detailed mechanistic investigation would be required to establish the exact cleavage mechanism for **23** and **24**, it is tempting to propose a rate-limiting step involving alkyl-oxygen heterolysis, in which an intermediate benzylic cation is stabilized by the electron-donating *para* substituent. A unimolecular fission pathway has been previously suggested for the thermal decomposition of a *p*-methoxybenzyl carbonate.[25]

Table 2. Kinetic parameters for rabbits 2509 and 2510 immunized five times with hapten **7**[a]

Rabbit #	Apparent K_M (μM)	Apparent V_{max} (μM/min)	% Hapten specific antibody	Apparent k_{cat}	Apparent k_{cat}/k_{uncat}
2509	34	0.27	10	9.6×10^{-2} min^{-1}	1430
2510	85	0.59	5.5	3.16×10^{-1} min^{-1}	4700

[a]Catalytic reactions utilized substrate **14**. The background rate for hydrolysis of **14** measured as k_{uncat} in the absence of polyclonal antibodies was 6.7×10^{-5} min^{-1}.

Table 3. Immunological and catalytic parameters determined for the polyclonal antibodies isolated from the BALB/cJ mice

	Hapten used to elicit BALB/cJ murine polyclonal antibodies				
	15	**16**	**17**	**18**	**19**
Titer[b]	1:800	1:800	1:800	1:1600	1:800
Apparent V_{max} (μM/min)[c]	0.12	0.068	0.0056	nd[a]	nd
Apparent K_M (μM)[c]	73	36	11	nm[a]	nm
Hapten specific antibody[d] total IgG	0.11	0.17	0.09	nm	nm
Apparent k_{cat} (min^{-1})[e]	0.045	0.017	0.016	nm	nm
Apparent k_{cat}/k_{uncat}[f]	1250	630	420	nm	nm

[a]nm, not measured; nd, none detected.
[b]Measured from standard ELISA using purified IgG at 1 mg/mL.
[c]Determined by Lineweaver–Burk analysis.
[d]Determined by quantitative inhibition studies.
[e]Calculated as apparent V_{max} divided by the amount of high-affinity, hapten specific antibody binding sites in the reactions.
[f]The values of k_{uncat} were determined under identical buffer conditions in the absence of added antibody. The k_{uncat} values of substrates **20**, **21**, and **22** were 3.6×10^{-5} min^{-1}, 2.7×10^{-5} min^{-1}, and 3.8×10^{-5} min^{-1}, respectively.

Apparent relative hapten dissociation constants (K_D) were determined using competition ELISA (Table 4). As expected, in each case, the polyclonal samples bound with highest affinity the hapten used to elicit them. By far the greatest specificity for hapten was seen with the antibodies elicited by hapten **15**, the 4-nitrobenzyl derivative. This result was not unexpected, as early in this century the pioneering studies of antibody cross-reactivity by Landsteiner[26] and Pauling and Pressman[27,28] showed that more electronegative groups, such as the nitro group, can dominate a high affinity antibody response.

To probe further the influences of animal species and strain upon the catalytic immune response, the KLH conjugates of haptens **15**–**18** were also used to immunize sets of 10 outbred ICR mice and pairs of New Zealand white rabbits. The immunization schedule followed was identical to that used for the BALB/cJ mice and the polyclonal samples were isolated from sera taken 10 days after the fifth and final immunization. A sample was also removed from the rabbits 10 days following the third immunization. The catalytic parameters of the polyclonal antibody samples for their most hapten-homologous substrates were determined as before and are shown in Table 5. The apparent k_{cat}/k_{uncat} values for the outbred ICR mice are about half as large, yet show the same trend of relative catalytic activities, as was seen with inbred BALB/cJ mice. Both rabbits immunized with **16** produced catalytic antibodies, and these antibodies displayed k_{cat}/k_{uncat} values similar to those of the murine samples. In contrast, none of the rabbits immunized with **15** or **17** produced catalytic antibodies following the full immunization schedule.

The K_D values obtained from the immunized rabbits and ICR mice are shown in Tables 6 and 7. Again, within a given sample, the highest affinity was seen for the hapten with which it was elicited. In general, the affinities seen with the polyclonal antibodies isolated from the ICR mice were similar or slightly better than those seen with the BALB/cJ mice, while the affinities measured for the samples from the rabbits were 3- to 40-fold higher than the murine samples.

Despite their lack of catalytic ability, the polyclonal antibodies elicited by haptens **15** and **17** in the rabbits did show a high degree of hapten affinity and specificity. Importantly, these polyclonal samples failed to show any significant binding to either their most hapten-homologous substrates, **20** and **22**, or the benzyl alcohol products that would result from the hydrolysis of these substrates (data not shown). Thus, it appears that the lack of observed catalysis elicited in these animals is due to a lack of substrate binding.

Catalytic parameters were also determined for the antibodies obtained from the rabbits 10 days following the third injection with haptens **15**–**17**. The apparent k_{cat}/k_{uncat} values of the anti-**16** rabbit samples were lower than the values observed with antibodies obtained

Table 4. Apparent dissociation constants, K_D (μM), for various haptens of BALB/cJ murine polyclonal antibodies as determined by competition ELISA[a]

BALB/cJ murine antibodies	Hapten				
	15	**16**	**17**	**18**	**19**
Anti-**15**	20 (±11)	>1000	>1000	>1000	>1000
Anti-**16**	50 (±10)	20 (±8.1)	400 (±180)	150 (±22)	>1000
Anti-**17**	300 (±180)	30 (±13)	5 (±1.8)	240 (±69)	400 (±170)
Anti-**18**	100 (±67)	30 (±16)	30 (±21)	0.5 (±0.3)	5 (±1.9)
Anti-**19**	>1000	700 (±260)	>1000	160 (±38)	1 (±0.48)

[a]Standard deviations of repetitive ELISA measurements are shown in parentheses.

Table 5. Immunological and catalytic parameters determined for the polyclonal antibodies isolated from the immunized ICR mice and the New Zealand white rabbits

	Hapten used to elicit polyclonal antibodies				
	15 (ICR)	**16** (ICR)	**17** (ICR)	**16** (NZW#3)	**16** (NZW#4)
Titer[a]	1:500	1:1000	1:800	1:800	1:900
Apparent V_{max} (μM/min)[b]	0.12	0.056	0.043	0.066	0.053
Apparent K_M (μM)[b]	28	23	52	9.3	13
Hapten specific antibody[c] total IgG	0.24	0.32	0.23	0.10	0.13
Apparent k_{cat} (min^{-1})[d]	0.021	0.0073	0.0078	0.028	0.017
Apparent k_{cat}/k_{uncat}[e]	580	270	200	1000	630

[a]Measured from standard ELISA using purified IgG at 1 mg/mL.
[b]Determined by Lineweaver–Burk analysis.
[c]Determined by quantitative inhibition studies.
[d]Calculated as apparent V_{max} divided by the amount of high-affinity, hapten specific antibody binding sites in the reactions.
[e]The values of k_{uncat} were determined under identical buffer conditions in the absence of added antibody. The k_{uncat} values of substrates **20**, **21**, and **22** were 3.6×10^{-5} min^{-1}, 2.7×10^{-5} min^{-1}, and 3.8×10^{-5} min^{-1}, respectively.

after five immunizations (Table 8). The K_D values for the same antibodies were slightly higher than those following the fifth injection. Surprisingly, the polyclonal antibodies isolated after the third injection from one of the two rabbits immunized with hapten **15** were slightly catalytic. The pseudo-first-order rate constant for the hydrolysis reaction of carbonate **20** in the presence of 12 μM anti-**15** polyclonal antibody was 3.9-fold higher than the pseudo-first-order rate constant found for the reaction in the absence of polyclonal antibodies. Unfortunately, this modest level of catalytic activity was not sufficient to allow a reliable determination of apparent catalytic parameters for the sample due to a low signal-to-noise ratio in the cleavage assay.

^{18}O labeling studies were used to investigate the rate-limiting step of the benzyl carbonate hydrolysis. If formation of the presumed tetrahedral intermediate is rate-limiting, then ^{18}O incorporation into substrate will not be observed, while if breakdown of the presumed tetrahedral intermediate is rate-limiting, then some substrate should be recovered that has ^{18}O incorporated as the carbonyl oxygen atom. Even after a 66 h incubation at pH 8.2 in 50% $H_2{}^{18}O$, mass spectral analysis of recovered substrate failed to show any incorporation of solvent oxygen into substrate **20** over the background level of isotopic oxygen, either in the presence or in the absence of rabbit anti-**15** antibodies. Using this technique, as little as 2% ^{18}O incorporation would have been detected.

Table 6. Apparent dissociation constants, K_D (μM), for various haptens of ICR murine polyclonal antibodies as determined by competition ELISA[a]

ICR murine antibodies	Hapten		
	15	**16**	**17**
Anti-**15**	2 (±0.71)	20 (±7.1)	>1000
Anti-**16**	20 (±6.9)	2 (±1.1)	200 (±92)
Anti-**17**	120 (±40)	5 (±1.9)	1 (±0.55)

[a]Standard deviations of repetitive ELISA measurements are shown in parentheses.

Discussion

The initial phase of the present work involved a series of enantiomeric hapten pairs, **1**–**6**, that were used to immunize New Zealand white rabbits. Enantiomeric pairs are ideal for use in systematic hapten structure–activity studies, because the two enantiomers have identical physical properties in achiral environments. Nevertheless, the stereoselectivity inherent in the immune response generally leads to two *different* immunological solutions to recognition, one for each enantiomer. In this way, the generality of any structure–activity relationship in the immune response can be gauged by comparing the results obtained with the pair of enantiomers.

For haptens **1**–**6**, the results of the immunizations were entirely self-consistent between enantiomers as well as among all the members of the set. In each case, a high affinity, stereoselective immune response was obtained judging from the ELISA studies (Table 1). The significant stereoselective preference for binding the immunizing hapten, as opposed to its enantiomer, indicates that the polyclonal responses were distinct for each enantiomer and that the hapten remained intact during the course of the immune response. Nevertheless, no catalytic activity was observed. These results are surprising, because **1**–**6** are similar in size to other phosphate and

Table 7. Apparent dissociation constants, K_D (μM), for various haptens of New Zealand white rabbit polyclonal antibodies as determined by competition ELISA[a]

Rabbit #/antibodies	Hapten		
	15	**16**	**17**
NZW#1/anti-**15**	0.05 (±0.009)	0.9 (±0.22)	>1000
NZW#2/anti-**15**	0.8 (±0.49)	40 (±26)	300 (±180)
NZW#3/anti-**16**	10 (±3.7)	0.6 (±0.24)	200 (±110)
NZW#4/anti-**16**	1 (±0.32)	0.4 (±0.27)	80 (±40)
NZW#5/anti-**17**	5 (±3.7)	2 (±0.86)	0.5 (±0.28)
NZW#6/anti-**17**	20 (±8.8)	2 (±1.4)	0.5 (±0.14)

[a]Standard deviations of repetitive ELISA measurements are shown in parentheses.

Table 8. Immunological and catalytic parameters determined for the polyclonal antibodies isolated from the New Zealand white rabbits immunized with hapten **16** following the third injection of hapten

	Anti-**16** third bleed antibody	
	Rabbit #3	Rabbit #4
Titer[a]	1:1250	1:2100
K_D (hapten, μM)[b]	1 (±0.42)	1.8 (±0.18)
Apparent V_{max} (μM/min)[c]	0.032	0.032
Apparent K_M (μM)[c]	9.3	39
Hapten specific antibody[d] total IgG	8.0	12
Apparent k_{cat} (min^{-1})[e]	0.017	0.011
Apparent k_{cat}/k_{uncat}[f]	620	410

[a]Measured from standard ELISA using purified IgG at 1 mg/mL.
[b]Determined by competition ELISA.
[c]Determined by Lineweaver–Burk analysis.
[d]Determined by quantitative inhibition studies.
[e]Calculated as apparent V_{max} divided by the amount of high-affinity, hapten specific antibody binding sites in the reactions.
[f]The values of k_{uncat} were determined under identical buffer conditions in the absence of added antibody. The k_{uncat} values of substrates **20**, **21**, and **22** were 3.6×10^{-5} min^{-1}, 2.7×10^{-5} min^{-1}, and 3.8×10^{-5} min^{-1}, respectively.

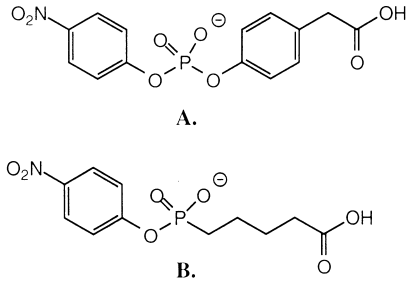

Scheme 3. (A) The structures of the hapten used by Gallacher and Brockelhurst et al.[1–3,5,10,11] to immunize sheep. (B) The structure of the hapten used by Suzuki et al.[7] to immunize rabbits.

phosphonate haptens that have been used previously to elicit catalytic antibodies.

It is unlikely that serendipity alone can explain the lack of catalytic activity elicited by haptens **1**–**6**, especially since pairs of enantiomers yielded the same results. Rather, there are probably structural features present in these six haptens that somehow prevent catalysis in the responding polyclonal antibodies. To emphasize this point, the rabbits originally immunized with haptens **3** and **4** were each immunized with hapten **7** as a positive control. Hapten **7** has been shown previously to elicit catalytically active polyclonal antibodies in rabbits as well as BALB/cJ mice. In both rabbits originally immunized with **3** and **4**, catalytic activity was present in the elicited polyclonal antibodies, and the observed apparent k_{cat}/k_{uncat} values of 1430 and 4700 compare well with the values obtained for other polyclonal samples immunized with this hapten. To the best of our knowledge, these are the first examples of animals being successfully reused for catalytic antibody studies.

The phosphate and phosphonate haptens investigated in this and previous polyclonal catalytic antibody studies can be divided into two distinct groups. Those haptens that have reproducibly generated antibody catalysts when used to immunize different animals, and those haptens that failed to elicit catalysts in repeated attempts, despite the presence of a high affinity immune response. Haptens in the first category include hapten **7**, used in this and previous studies,[9,13] the nitrophenyl phosphate hapten of Gallacher and Brocklehurst et al.[1–3,5,10,11] (hapten 'A' in Scheme 3), and the nitrophenyl phosphate hapten of Suzuki et al.[7] (hapten 'B' in Scheme 3). Haptens in the latter category include haptens **1**–**6**.

It can be argued from the negative catalytic results for haptens **1**–**6** that a change associated with altered leaving group ability/structure and/or location may be responsible for the observed differences in elicited catalytic activities. Haptens **1**–**6** and the haptens used to elicit successfully catalytic activity are of a similar size, and haptens **1**, **2** and **5**, **6** have phenyl rings on both sides of the phosphonate or phosphate moiety, respectively, just like the successful haptens. One difference between successful and unsuccessful haptens involves the nature of the leaving group on corresponding substrates. Corresponding substrates for the successful haptens have relatively good leaving groups, phenyl or 4-nitrophenyl, while corresponding substrates for the unsuccessful haptens have 4-alkylphenyl (more electron rich compared to phenyl or 4-nitrophenyl) or benzyl leaving groups. Perhaps these differences in leaving group lead to differences in rate-limiting transition state structure (see 'Mechanistic considerations' below). Another clear difference is that the successful haptens have phenyl or 4-nitrophenyl groups located on the side of the hapten opposite the linker, while the unsuccessful haptens **1**–**6** have more flexible alkyl or benzyl groups in the analogous position. Note that attention is being paid to the location of the group with respect to the linker, since it is generally observed that groups farthest from the linker dominate the immune response and are buried most deeply in the elicited antibody binding pockets. This is not surprising given that linkage to a carrier protein introduces obvious steric hindrance to binding of nearby groups, thereby limiting antibody interactions in this region of the hapten.

If altered leaving group ability/location and/or hapten flexibility are important, then benzyl haptens **15**–**19** would also be predicted to be less likely to elicit antibody catalysts than a phenyl hapten such as **7**; and, indeed, both in terms of the level of observed catalytic activity, as well as frequency of elicited catalysts, the haptens **15**–**19** proved to be significantly less effective than hapten **7**. Benzyl haptens **15**–**17** elicited catalysts that were only moderately active, having apparent k_{cat}/k_{uncat} values between 0 and 1250 in all the animal systems examined. This compares to apparent k_{cat}/k_{uncat} values between 1400 and 40,000 seen with the phenyl hapten **7**.[9,13] Importantly, out of the three separate studies using a total of five rabbits and 10 mice immunized with hapten **7** that have now been completed, catalytic activity was observed in *each* case, while the benzyl haptens **3**, **4**, **15**, and **17** failed to elicit catalytic activity after five immunizations in any of the rabbits used. At

this time, it is not clear why the 4-chlorobenzyl hapten **16** should elicit catalysts in the rabbits, while the 4-nitrobenzyl (**15**) and underivatized benzyl (**17**) haptens did not.

Mechanistic considerations

One possible mechanistic explanation for the differences seen between the successful and less successful hapten systems involves a difference in rate-limiting step for phenyl carbonate substrates such as **14** compared to the benzyl carbonate substrates such as **20**–**22**. The phenolate anion is a better leaving group than a benzyloxy anion, judging from the rate constants for the hydrolyses of the benzyl carbonate substrates measured in the absence of antibody. The benzyl carbonates **20**–**22** hydrolyzed with rate constants ranging from 3.8×10^{-5} min^{-1} to 2.7×10^{-5} min^{-1}, while the hydrolysis rate constant for the phenyl carbonate **14** was 5×10^{-5} min^{-1} when measured at the same pH. Thus, even though these rate differences are small, it is theoretically possible that for a phenyl carbonate such as **14**, formation of the tetrahedral intermediate could be rate-limiting, while the more sluggish benzyloxy leaving groups could change the rate-limiting step to breakdown of the tetrahedral intermediate for **20**–**22**. Such a change in rate-limiting step could explain differences in behavior between antibodies elicited by phenyl phosphates versus benzyl phosphates. Yet, the ^{18}O labeling studies found no incorporation of ^{18}O into substrate **20** even after extended incubation, sufficient for substantial hydrolysis, *with or without* antibody. Thus, there is no reason to believe that the rate-limiting step of the hydrolysis reaction has changed to breakdown of the tetrahedral intermediate for the benzyl systems, at least for **20**, either in solution or in the antibody binding pocket. Of course, there is no way to rule out more subtle differences in mechanism such as the detailed geometry of the rate-limiting transition state that may be different between phenyl and benzyl carbonates, leading to differences in antibody catalysis.

Another mechanistic question that deserves comment involves substrates **23** and **24**. The lack of pH dependence for the hydrolysis of substrates **23** and **24** in the absence of antibody (see Fig. 1) indicates that these substrates react by a mechanism different from the $B_{AC}2$ mechanism presumed for the other carbonate substrates of this study. It is gratifying that no catalysis was observed with these substrates for any of the antibodies elicited in BALB/cJ mice by **15**–**19**. Interestingly, the antibodies elicited by haptens **18** and **19** were catalytic for hydrolysis of substrates **20**–**22**, the substrates that showed the pH dependence of reaction expected for the $B_{AC}2$ mechanism. Thus, the importance of transition state stabilization has been clearly identified within this system of haptens and substrates.

Different species

The differences seen between species immunized with haptens **15**–**17** are interesting. In general, the murine

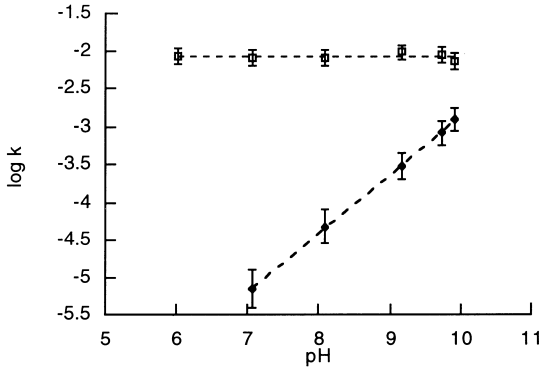

Figure 1. pH Dependence of the hydrolysis reactions of carbonates **22** and **23**. The open squares represents points for carbonate **23**, the darkened diamonds represent points for carbonate **22**. The pH independence of hydrolysis for carbonate **23** was taken as evidence for a mechanism other than $B_{AC}2$. Substrates **20** and **21** behaved in a manner analogous to **22**, while substrate **24** behaved in a manner analogous to **23**. These were omitted for clarity.

immune responses were of significantly lower hapten affinity compared to those seen with the rabbits. In addition, with haptens **15** and **17**, the rabbits displayed high hapten affinity, but no catalysis after five immunizations in all of the rabbits used. Both species of mice produced moderately active catalysts with these haptens. We were unable to analyze catalytic activity in individual mice because of small serum volumes, so it is currently unknown how catalytic activity varied in the different mice.

Flexibility

While other explanations such as pure serendipity (presumably unlikely given the large number of experiments described here) or subtle changes in transition-state structure cannot and should not be ruled out, an intriguing idea is that flexibility in the region of the hapten opposite the linker decreases effectiveness in the less successful haptens **1**–**6** and **15**–**17**. An aspect of flexible systems that could decrease catalytic antibody activity is that antibody-bound conformations of the flexible haptens may be different than any relatively low-energy conformation obtainable by a flexible substrate. This appears to be the case for at least the rabbit antibodies elicited by haptens **15** and **17**, since these antibodies displayed no binding to their most homologous substrates within the limits of the competition ELISA. Interestingly, these non-catalytic rabbit antibodies to **15** and **17** were of higher affinity to the immunizing hapten than the catalytic responses generated in mice, possibly indicating that the higher affinity antibodies are less 'forgiving.' Nevertheless, other non-catalytic polyclonal samples in our studies did bind substrate, indicating that there is likely more to be considered than a lack of substrate binding.

Flexibility of the hapten could conceivably disrupt catalysis of a bound substrate in other ways. For example, a flexible hapten could elicit an antibody binding pocket that can bind substrates, but in a ground state conformation that cannot proceed to transition state(s)

and/or products due to conformational constraints. For example, flexible haptens may 'collapse' due to hydrophobic factors, etc., into low energy structures that are then recognized by antibodies. These collapsed conformations recognized by the antibodies may not be compatible with catalysis along the *entire* reaction coordinate. Note that these flexibility arguments may fit nicely with those presented by Linder et al.[29] in which rearrangment of the binding pocket to an 'active' form was required for catalysis in a series of benzyl ester hydrolyzing antibodies.

Conclusion

Antibody catalysis is a complex phenomenon, and studies with numerous haptens, such as those described here, are required to establish important trends that may not be obvious from any one study. Taken together, our data indicate that some haptens produce immune responses that are reproducibly highly catalytic, while seemingly similar haptens produce immune responses that are reproducibly less catalytically active. Whatever the explanation, subtle changes in mechanistic features due to altered leaving group ability/location or overall hapten flexibility, the comprehensive data presented here indicate that phenyl or 4-nitrophenyl leaving groups located opposite the hapten linker are to be preferred in order to elicit highly active antibody catalysts for acyl hydrolysis reactions. This work complements our previous studies which demonstrated that large, hydrophobic groups should be avoided when designing transition state analogue haptens,[13] and that homology between hapten and substrate is important.[12] Future studies will hopefully validate and refine these emerging rules for the production of optimized transition state analogue haptens.

Experimental

Syntheses

***N*-CBZ-1-aminoethylphosphonic acid, (4-carboxy)benzyl ester (1 and 2).** Both enantiomers were prepared according to the following procedure. 1-aminoethylphosphonic acid (0.5 g, 4 mmol) was dissolved in 10 mL of 10% Na_2CO_3 (aq). An excess of benzylchloroformate (1.02 g, 6 mmol) in 3 mL of tetrahydrofuran (THF) was added and the reaction was allowed to stir at room temperature for 4 h. Vigorous bubbling of the solution was observed. The excess benzylchloroformate and impurities were removed by extraction into diethyl ether and the resulting aqueous layer acidified to pH 2 with hydrochloric acid. The aqueous layer was extracted three times with diethyl ether. The combined organic extracts were dried over sodium sulfate, filtered, and the solvents removed on the rotary evaporator to yield colorless crystals of *N*-CBZ-1-aminoethylphosphonic acid. A portion of the acid (0.4 g, 1.54 mmol) was dissolved in 9 mL of *N,N*-dimethylformamide (DMF), blanketed with argon, and chilled to −20 °C. Thionyl chloride (0.38 g, 3.17 mmol) was added via syringe and the reaction stirred at −20 °C for 5 min. The reaction mixture was allowed to warm to −5 °C and stirred for an additional 20 min followed by stirring at room temperature for 20 min. Methyl-4-hydroxymethylbenzoate (0.25 g, 1.54 mmol) dissolved in 2 mL DMF was added and the reaction was allowed to warm to room temperature where it was stirred for 4 h. Saturated sodium bicarbonate (10 mL) was added and the reaction mixture was washed twice with diethyl ether. The resulting aqueous layer was purified by ion affinity chromatography on DEAE Sephadex A-25, using 100 mM potassium chloride as eluent. The aqueous solvents were removed in vacuo and the resulting white solid was purified on a short column of silica gel, eluting with 10% methanol in ethanol. The solvents were removed on the rotary evaporator, resulting in a white solid. This solid, *N*-CBZ-1-aminoethylphosphonic acid, (4-methoxycarbonyl)-benzyl ester, potassium salt (0.105 g, 0.26 mmol) was dissolved in water/THF/methanol. The ratio of solvents was adjusted until the solution was homogeneous. One equivalent of lithium hydroxide (0.012 g, 0.26 mmol) was added and the reaction stirred at 60 °C for 4 h. The solvents were removed on the rotary evaporator. The resulting crude product was purified by reversed-phase liquid chromatography, eluting with a 1-h gradient from 100% water to 100% acetonitrile. The solvents were removed in vacuo to yield a white powder. ^{1}H NMR (300 MHz, D_2O) δ_H 1.30 (3H, dd, $J = 17.9$, 8.5 Hz, $CHCH_3$), 3.85 (1H, m, $CHCH_3$), 4.95 (4H, complex multiplet, both $ArCH_2$), 7.35, (5H, m, C_6H_5O), 7.41 (2H, d, $J = 12.6$ Hz, Ar*H*), 7.85 (2H, d, $J = 9.5$ Hz, Ar*H*); ^{13}C NMR (300 MHz, D_2O) δ_C 11.86, 16.13, 52.57, 66.99, 67.07, 126.42, 127.25, 127.46, 128.58, 129.98, 130.36, 139.75, 142.20, 142.30, 156.92, 166.88; high-resolution FABMS calcd for $C_{18}H_{18}NO_7P$: 391.0821, found 391.0204; mp > 250 °C (uncorr).

***N*-Methoxycarbonyl-1-aminoethylphosphonic acid, (4-carboxy)benzyl ester (3 and 4).** Both enantiomers were prepared according to the following procedure. 1-Aminoethylphosphonic acid (0.33 g, 2.64 mmol) was dissolved in an excess of 10% Na_2CO_3 (aq). An excess of methyl chloroformate (0.38 g, 4 mmol) in 2 mL of tetrahydrofuran (THF) was added and the reaction was allowed to stir at room temperature for 4 h. Vigorous bubbling of the solution was observed. The excess methylchloroformate and solvents were removed in vacuo resulting in a crystalline, white solid. *N*-methoxycarbonyl-1-aminoethylphosphonic acid, disodium salt (0.6 g, 2.64 mmol) was dissolved in 9 mL of *N,N*-dimethylformamide (DMF), blanketed with argon, and chilled to −20 °C. Thionyl chloride (0.38 g, 3.17 mmol) was added via syringe and the reaction stirred at −20 °C for 5 min. The reaction mixture was allowed to warm to −5 °C and stirred for an additional 20 min followed by stirring at room temperature for 20 min. Methyl-4-hydroxymethylbenzoate (0.44 g, 2.64 mmol) dissolved in 2 mL DMF was added and the reaction was allowed to warm to room temperature where it was stirred for 4 h. Saturated sodium bicarbonate (10 mL) was added and the reaction mixture was washed twice with diethyl ether. The resulting aqueous layer was purified by ion affinity chromatography on DEAE Sephadex A-25,

using 100 mM potassium chloride as eluent. The aqueous solvents were removed in vacuo and the resulting white solid was purified on a short column of silica gel, eluting with 10% methanol in ethanol. The solvents were removed on the rotary evaporator, resulting in a white solid. This salt, *N*-methoxycarbonyl-1-aminoethylphosphonic acid, (4-methoxycarbonyl)benzyl ester, potassium salt (0.48 g, 1.3 mmol) was dissolved in water/THF/methanol. The ratio of solvents was adjusted until the solution was homogeneous. One equivalent of lithium hydroxide (0.055 g, 1.3 mmol) was added and the reaction stirred at 60 °C for 4 h. The solvents were removed on the rotary evaporator. The resulting crude product was purified by reversed-phase liquid chromatography, eluting with a 1 h gradient from 100% water to 100% acetonitrile. The solvents were removed in vacuo to yield a white powder. ^{1}H NMR (300 MHz, D_2O) δ_H 1.34 (3H, dd, $J=16.7$, 7.3 Hz, CHCH_3), 3.80 (3H, s, CH_3O), 3.85 (1H, m, CHCH$_3$), 5.06 (2H, d, $J=7.22$ Hz, ArCH_2), 7.38 (2H, d, $J=9.81$ Hz, ArH), 7.93 (2H, d, $J=8.26$ Hz, ArH); ^{13}C NMR (300 MHz, D_2O) δ_C 11.23, 16.13, 52.32, 52.57, 66.99, 67.07, 127.46, 129.98, 130.36, 142.20, 142.30, 156.83, 156.92, 166.88; high-resolution FABMS calcd for $C_{12}H_{14}NO_7P$: 315.0508, found 315.0996; mp >250 °C (uncorr).

***O*-1-Phenylpropyl-*O*-(4-carboxymethylphenyl)-phosphate, tetrabutylammonium salt, lithium salt (5 and 6).** Both enantiomers were prepared using a procedure adopted from Martin and Josey[30] using (trimethylsilyl)ethyl phosphite, prepared according to the method of Poulter et al.[31] 7.55 g (55 mmol) of PCl_3 was dissolved in 60 mL dry ether and chilled to −78 °C under argon. 5 g (42 mmol) of 2-(trimethylsilyl)ethanol in 80 mL dry ether were added slowly using a cannula. The reaction was stirred at −78 °C for 1 h and then allowed to come to room temperature. The solvents were removed at reduced pressure on the rotary evaporator, care being taken to exclude moisture. The clear residue was distilled under high vacuum. The fraction boiling at 38–40 °C was collected in a chilled flask (−78 °C). The flask was sealed with a septum and blanketed with argon. The clear, liquid 2-(trimethylsilyl)ethyl dichlorophosphite was stored at 4 °C 1.15 g (5.65 mmol) 2-(trimethylsilyl)ethyl dichlorophosphite were added to a dry flask using a tared syringe. Dry THF was added and the solution chilled to −78 °C under argon. 1.83 g (14 mmol) of dry diisoproplyethylamine were added to the solution followed by 0.83 g (5 mmol) of methyl-4-hydroxyphenylacetate dissolved in dry THF. A white precipitate formed. The reaction was stirred for 10 min. 0.77 g (5.65 mmol) of 1-phenyl-1-propanol dissolved in dry THF were added. The reaction was stirred at −78 °C for 2 h, removed from the cooling bath, and stirred for an additional hour. Solvents were removed on the rotary evaporator and the residue taken up in ethyl acetate. This solution was filtered through Celite 545, dried over sodium sulfate, filtered, and the solvents removed on the rotary evaporator. The resulting crude phosphite was purified on silica gel (hexane:ethyl acetate, 80:20). The phosphite was dissolved in dichloromethane and 0.29 g (1 mL, 8.48 mmol) of 30% H_2O_2 was added slowly. The reaction was allowed to stir at room temperature for 2 h. The reaction mixture was poured into saturated NaCl and washed twice. The organic layer was dried over sodium sulfate, filtered, and the solvents removed on the rotary evaporator (procedure in ref 8) The crude phosphates were purified on silica gel, eluting with 20% ethyl acetate:80% hexane to yield a colorless oil. 1.0 M tetrabutyl ammonium fluoride in THF (1.1 equiv, according to the weight of the phosphate recovered) was added to a solution of the purified phosphate and allowed to stir at room temperature until bubbling ceased. To this solution was added one equivalent of LiOH in 1:1 methanol:water and the reaction stirred overnight at room temperature. Solvents were removed to yield the hapten as a light-yellow solid. ^{1}H NMR (250 MHz, D_2O) δ_H 0.70 (3H, t, $J=8.6$ Hz, CH_3-CH$_2$CH), 0.81 (12H, t, $J=8.6$ Hz, CH_3CH$_2$CH$_2$CH$_2$), 1.23 (8H, m, $J=11.5$ Hz, CH$_3$CH_2CH$_2$CH$_2$), 1.49 (8H, m, CH$_3$CH$_2$CH_2CH$_2$), 1.75 (2H, m, $J=5.7$ Hz, CH$_3$-CH_2CH), 3.04 (8H, t, CH$_3$CH$_2$CH$_2$CH_2), 4.90 (1H, q, $J=8.6$ Hz, CH$_3$CH$_2$CH), 6.75 (2H, d, $J=11.5$ Hz, ArH), 6.95 (2H, d, $J=9.8$ Hz, ArH), 7.24 (5H, m, C_6H_5); ^{13}C NMR (300 MHz, D_2O) δ_C 9.55, 14.0, 20.2, 24.7, 33.2, 41.2, 59.5, 70.0, 121.1, 121.3, 126.2, 127.2, 127.6, 128.5, 128.9, 130.1; high-resolution FABMS calcd for $C_{33}H_{53}NO_6PLi$: 597.3770, found 597.7062; mp >280 °C (uncorr).

***O*-4-Carboxybenzyl-*O*-phenylphosphate, lithium salt, tetrabutyl ammonium salt (7).** The procedure above was followed using phenol and methyl-4-hydroxymethylbenzoate as the two alcohols added to the 2-(trimethylsilyl)ethyl dichlorophosphite to yield the hapten as a white solid. ^{1}H NMR (300 MHz, CD_3OD) δ_H 1.02 (12H, t, $J=9$ Hz, CH_3CH$_2$CH$_2$CH$_2$) 1.38 (8H, sextet, $J=9$ Hz, CH$_3$CH_2CH$_2$CH$_2$), 1.64 (8H, quintet, $J=10$ Hz, CH$_3$CH$_2$CH_2CH$_2$), 3.23 (8H, t, $J=12$ Hz, CH$_3$CH$_2$CH$_2$CH_2), 5.00 (2H, d, $J=9$ Hz, ArCH_2), 7.00–7.26 (5H, m, C_6H_5), 7.32 (2H, d, $J=9$ Hz, ArH), 7.89 (2H, d, $J=9$ Hz, ArH); ^{13}C NMR (300 MHz, CD_3OD) δ_C 13.98, 20.64, 24.72, 59.38, 68.22, 68.28, 121.23, 121.30, 124.11, 127.51, 130.16, 130.30, 138.25, 141.45, 141.50, 154.46, 154.51, 174.73; high-resolution FABMS calcd for $C_{14}H_{11}O_6PLi$: 313.0453, found 313.0443; mp >280 °C (uncorr).

***N*-(2-diethylaminoethyl)-4-hydroxymethylbenzamide.** To a stirred solution of 4-hydroxymethyl benzoic acid pentafluorophenyl ester (Sigma) (1.5 g, 4.7 mmol) in dichloromethane at 0 °C were added 0.66 g (5.7 mmol) of 2-(diethylamino)ethylamine. The resulting solution was stirred at 0 °C for 30 min and allowed to warm to room temperature for an additional 30 min. The reaction mixture was washed three times with 1 N NaOH, once with saturated NaCl, dried over sodium sulfate, and filtered. The solvents were removed on the rotary evaporator and the resulting pale, brown oil was placed under high vacuum overnight. The oil was chromatographed on silica (10% methanol:methylene chloride) to yield a pale-yellow oil. ^{1}H NMR (300 MHz, CD_2Cl_2) δ_H 1.01 (6H, t, $J=7.2$ Hz, CH_3CH$_2$), 2.57 (4H, q, $J=7.2$ Hz, CH$_3$CH_2), 2.65 (2H, t, $J=6.1$ Hz, NCH_2 CH$_2$NH), 3.42 (2H, q, $J=5.8$ Hz, NCH$_2$CH_2NH), 4.65 (2H, s, ArCH_2), 7.25 (2H, d, $J=8.1$ Hz, ArH), 7.65 (2H,

d, $J=7.8$ Hz, Ar*H*); ^{13}C NMR (300 MHz, CD_2Cl_2) δ_C 11.62, 37.64, 47.04, 51.97, 63.89, 126.77, 127.25, 133.55, 145.63, 167.70; high-resolution MS (CI+) calcd for $C_{14}H_{23}N_2O_2$ (MH^+): 251.1760, found 251.1764.

***N*-CBZ-alanine, *N*-(2-diethylaminoethyl)-4-hydroxymethylbenzamide ester (8 and 9).** Both enantiomers were produced as follows. Alanine (3 g, 34 mmol) was dissolved in an excess of 10% Na_2CO_3 (aq). An excess of benzylchloroformate in tetrahydrofuran (THF) was added and the reaction was allowed to stir at room temperature for 4 h. Vigorous bubbling of the solution was observed. The excess benzylchloroformate and impurities were removed by extraction into ethyl acetate and the resulting aqueous layer dried in vacuo, resulting in a crystalline, white solid. The solid was dissolved in water and the resulting solution made acidic with 0.1 M HCl and extracted three times with ethyl acetate. The combined organic extracts were dried over sodium sulfate, filtered, and the solvents removed on the rotary evaporator to yield a white solid. The *N*-CBZ-alanine (0.52 g, 23.5 mmol) was dissolved in DMF/dichloromethane and 4-hydroxybenzotriazole (HOBt) (0.32 g, 23.5 mmol) in DMF was added followed by dicyclohexylcarbodiimide (DCC) (0.49 g, 23.5 mmol). The reaction was stirred under argon for 1 h at room temperature. A solution of *N*-(2-diethylaminoethyl)-4-hydroxymethylbenzamide (0.59 g, 23.5 mmol) in dichloromethane was added. The reaction mixture was allowed to stir at room temperature for 4 h and then filtered to remove the precipitated dicyclohexylurea. The solvents were removed by vacuum distillation and the resulting residue extracted with ethyl acetate. The combined ethyl acetate layers were dried over sodium sulfate, filtered, and the solvents removed on the rotary evaporator. The substrate was purified by column chromatography on silica gel using 2% methanol in dichloromethane as eluent to yield a thick, tan colored oil. ^{1}H NMR (300 MHz, CD_2Cl_2) δ_H 1.01 (6H, t, $J=7.2$ Hz, CH_3CH$_2$), 1.41 (3H, d, $J=7.2$ Hz, CH$_3$CH), 2.54 (4H, q, $J=5.7$ Hz, CH$_3$CH_2), 2.61 (2H, t, $J=6.0$ Hz, NCH_2CH$_2$NH), 3.43 (2H, q, $J=5.7$ Hz, NCH$_2$CH_2NH), 4.39, (1H, m, CH$_3$C*H*), 5.07 (2H, s, ArCH_2), 5.18 (2H, s, ArCH_2), 6.17 (1H, d, $J=7.5$ Hz, NH), 7.25 (1H, m, NH), 7.32 (5H, m, C$_6H_5$), 7.37 (2H, d, $J=8.1$ Hz, Ar*H*), 7.78 (2H, d, $J=8.2$ Hz, Ar*H*); ^{13}C NMR (300 MHz, CD_2Cl_2) δ_C 13.5, 18.8, 38.7, 46.6, 50.2, 52.3, 67.5, 68.3, 127.0, 127.5, 128.2, 128.7, 129.0, 129.4, 135.1, 139.9, 163.5, 166.3, 174.7; high-resolution MS (CI+) calcd for $C_{25}H_{33}N_3O_5$: 455.2420, found 455.5589.

***N*-Methoxycarbonylalanine, *N*-(2-diethylaminoethyl)-4-hydroxymethylbenzamide ester (10 and 11).** Both enantiomers were produced as follows. Alanine (2 g, 22 mmol) was dissolved in an excess of 10% Na_2CO_3 (aq). An excess of methyl chloroformate (4.2 g, 45 mmol) in THF was added and the reaction was allowed to stir at room temperature for 4 h. Vigorous bubbling of the solution was observed. The excess methylchloroformate and solvents were removed in vacuo resulting in a crystalline, white solid. The solid was dissolved in water and the resulting solution made acidic with 0.1 M HCl and extracted three times with ethyl acetate. The combined organic extracts were dried over sodium sulfate, filtered, and the solvents removed on the rotary evaporator to yield a colorless oil. The *N*-methoxycarbonylalanine (0.5 g, 3.4 mmol) was dissolved in DMF/dichloromethane and HOBt (0.46 g, 3.4 mmol) in DMF was added followed by DCC (0.7 g, 3.4 mmol). The reaction was stirred under argon for 1 h at room temperature. A solution of *N*-(2-diethylaminoethyl)-4-hydroxymethylbenzamide (0.85 g, 3.4 mmol) in dichloromethane was added. The reaction mixture was allowed to stir at room temperature for four hours and then filtered to remove the precipitated urea. The solvents were removed by vacuum distillation and the resulting residue extracted with ethyl acetate. The combined ethyl acetate layers were dried over sodium sulfate, filtered, and the solvents removed on the rotary evaporator. The substrate was purified by column chromatography on silica gel using 2% methanol in dichloromethane as eluent, giving a colorless oil. ^{1}H NMR (300 MHz, CD_2Cl_2) δ_H 1.01 (6H, t, $J=7$ Hz, CH_3CH$_2$), 1.41 (3H, d, $J=7.2$ Hz, CH$_3$CH), 2.57 (4H, q, $J=5.7$ Hz, CH$_3$CH_2), 2.65 (2H, t, $J=6$ Hz, NCH_2CH$_2$NH), 3.42 (2H, q, $J=6$ Hz, NCH$_2$CH_2NH), 3.64 (3H, s, CH_3O), 4.40 (1H, m, CH$_3$C*H*), 5.22 (2H, s, ArCH_2), 5.39, (1H, d, $J=7$ Hz, NH), 7.25 (2H, d, $J=8$ Hz, Ar*H*), 7.65 (2H, d, J 8.2 Hz, Ar*H*); ^{13}C NMR (300 MHz, CD_2Cl_2) δ_C 11.62, 18.26, 37.64, 47.04, 49.37, 51.97, 52.38, 63.89, 126.77, 127.25, 133.55, 145.63, 156.61, 167.70, 177.03; High-resolution MS (CI+) calcd for $C_{19}H_{29}N_3O_5$: 379.2107, found 379.4600.

(4-(*N*-Butyl) carboxamidomethyl) phenyl (1-phenyl)-1-propyl carbonate (12 and 13). Both enantiomers were prepared as follows. 4-Nitrophenylchloroformate (1.9 g, 6.3 mmol) was dissolved in dry dichloromethane and blanketed with argon while being chilled to 0 °C in an ice/water bath. 0.51 mL (6.3 mmol) of dry pyridine was added via syringe and a precipitate formed. This was followed by the dropwise addition of 0.77 g (5.65 mmol) of 1-phenyl-1-propanol. The reaction mixture cleared. The reaction was stirred for 4 h while warming to room temperature. During this time a precipitate formed. The solvents were removed in vacuo. The crude reaction mixture was chromatographed on silica gel (CH_2Cl_2) yielding a tan colored solid. *N*-Butyl-4-hydroxyphenylacetamide (0.43 g, 2.2 mmol) was dissolved in dry THF and blanketed with argon while chilling to 0 °C. 0.053 g (2.2 mmol) of NaH was added. The reaction mixture bubbled vigorously. After the bubbling subsided, 0.66 g (2.2 mmol) 1-phenyl-1-propyl 4-nitrophenyl carbonate in THF was added via syringe and the reaction mixture allowed to warm to room temperature over 2 h, during which time the reaction mixture turned bright yellow. The solvents were removed on the rotary evaporator and the yellow residue was dissolved in ethyl acetate and washed with 1% NaOH until the aqueous extracts were colorless. The organic layer was washed with water followed by saturated NaCl. The organic layer was dried over sodium sulfate, filtered, and the solvents removed on the rotary evaporator. The resulting oil was chromatographed on silica gel (2% methanol/dichloromethane) to yield a colorless oil. ^{1}H NMR (300 MHz, CD_2Cl_2) δ_H 0.92 (6H, complex multiplet, CH_3), 1.39

(2H, m, $J=6.9$ Hz, $CH_3CH_2CH_2CH_2$), 1.58 (2H, m, $J=7.1$ Hz, $CH_3CH_2CH_2CH_2$), 2.00 (2H, complex multiplet, $CHCH_2CH_3$), 3.41 (2H, q, $J=7.0$ Hz, $CH_3CH_2CH_2CH_2$), 3.61 (2H, s, $ArCH_2$), 5.6 (1H, t, $J=7.4$ Hz, $CHCH_2CH_3$), 6.20 (1H, s, NH), 7.09 (2H, d, $J=9.5$ Hz, ArH), 7.25 (2H, d, $J=9.7$ Hz, ArH), 7.40 (5H, m, C_6H_5); ^{13}C NMR (300 MHz, CD_2Cl_2) δ_C 9.97, 29.70, 40.61, 52.28, 82.82, 121.48, 126.85, 128.60, 128.85, 130.70, 132.50, 140.1, 150.7, 154.0, 172.0; high-resolution MS calcd for $C_{21}H_{26}NO_5$ (MH^+): 372.1733, found 372.4371.

4-(*N*-(2-(Diethylamino)ethyl)carbamoyl)benzyl phenyl carbonate (14). *N*-(2-Diethylaminoethyl)-4-hydroxymethylbenzamide (0.48 g, 1.93 mmol) was dissolved in dry dichloromethane and blanketed with argon while being chilled to 0 °C in an ice/water bath. 0.15 mL (1.93 mmol) of dry pyridine was added via syringe followed by the dropwise addition of 0.28 mL (2.31 mmol) of phenyl chloroformate. The reaction was stirred for 4 h while warming to room temperature. The reaction mixture was then washed three times with 0.1 M NaOH followed by one wash with saturated NaCl. The organic phase was dried over sodium sulfate, filtered, and the solvents removed at reduced pressure. The crude carbonate was chromatographed on silica gel using 2% methanol in dichloromethane as eluent. The resulting pale brown oil was stored in vacuo overnight: ^1H NMR (300 MHz, CD_2Cl_2) δ_H 0.92 (6H, t, $J=7.2$ Hz, CH_3CH_2), 2.55 (4H, q, $J=7.0$ Hz, CH_3CH_2), 2.54 (2H, t, $J=6.2$ Hz, NCH_2CH_2NH), 3.36 (2H, q, $J=5.7$ Hz, NCH_2CH_2NH), 5.17 (2H, s, $ArCH_2$), 7.07 (2H, d, $J=7.6$ Hz, ArH), 7.24 (5H, m, C_6H_5) 7.45 (2H, d, $J=8.1$ Hz, ArH); ^{13}C NMR (300 MHz, CD_2Cl_2) δ_C 11.97, 37.71, 47.10, 51.80, 69.78, 121.35, 126.42, 127.60, 128.42, 129.79, 135.42, 138.43, 151.47, 153.86, 166.80; HRMS (CI+) calcd for $C_{21}H_{27}N_2O_4$ (MH^+): 371.1971, found 371.1963.

4-(Carboxy)phenylmethyl 4-nitrophenylmethyl phosphate, dipotassium salt (15). The procedure for making haptens **5** and **6** was followed, using 4-nitrobenzyl alcohol and methyl 4-(hydroxymethyl)benzoate as the two alcohols added to the 2-(trimethylsilyl)ethyl dichlorophosphite, excepting that after removal of the silyl protecting group with tetrabutyl ammonium fluoride, the resulting residue was dissolved in H_2O and loaded onto DEAE Sephadex A-25 anion exchange resin. The resin was washed with H_2O and then the phosphate was eluted with 150 mM KCl. The H_2O was lyophilized to leave behind a copious amount of white powder. A mixture of 10% methanol in ethanol was added to the powder to make a slurry which was filtered through silica gel to remove excess KCl. The concentrated filtrate was taken up in ethanol and filtered through a fritted glass funnel to remove any silica gel which may have dissolved in the methanol/ethanol mixture. The residue left after concentration of this second filtrate was dissolved in 30 mL methanol, and 1 M aq KOH (0.892 mL, 0.892 mmol) was added. The resulting mixture was stirred at room temperature overnight. Solvent was removed by rotary evaporator to afford the hapten as a olive green solid. ^1H NMR (250 MHz, CD_3OD) δ_H 4.92 (4H, m, $ArCH_2$), 7.33 (2H, m, ArH), 7.55 (2H, m, ArH), 7.88 (2H, m, ArH), 8.15 (2H, m, ArH); ^{13}C NMR (250 MHz D_2O) δ_C 67.0 (d, $J=6$ Hz); 68.0 (d, $J=6$ Hz); 124.3; 127.8; 128.0; 128.4; 129.7 (d, $J=6$ Hz); 136.5; 140.7; 145.8; 175.7; high-resolution FABMS calcd for $C_{15}H_{13}NO_8P$: 366.0379, found 366.0364.

4-(Carboxy)phenylmethyl 4-chlorophenylmethyl phosphate, dipotassium salt (16). The procedure described above for **15** was followed using 4-chlorobenzyl alcohol in place of the 4-nitrobenzyl alcohol, yielding the hapten as a white solid. ^1H NMR (250 MHz, CD_3OD) δ_H 4.87 (4H, m, $ArCH_2$), 7.33 (6H, m, ArH), 7.93 (2H, d, $J=4$ Hz, ArH); ^{13}C NMR (250 MHz, D_2O) δ_C 67.3 (d, $J=5$ Hz); 68.0 (d, $J=5$ Hz); 127.9; 129.2; 129.8; 130.0; 134.0; 136.6; 140.8; 141.0; 175.9; high-resolution FABMS for $C_{15}H_{13}O_6PCl$: calcd 355.0138, found 355.0115.

4-(Carboxy)phenylmethyl phenylmethyl phosphate, dipotassium salt (17). The procedure described for **15** was followed using benzyl alcohol in place of the 4-nitrobenzyl alcohol, affording the hapten as a white solid. ^1H NMR (250 MHz, CD_3OD) δ_H 4.89 (4H, m, $ArCH_2$), 7.32 (7H, m, ArH), 7.92 (2H, m, ArH); ^{13}C NMR (250 MHz, D_2O) δ_C 68.0 (d, $J=6$ Hz); 69.0 (d, $J=5$ Hz); 128.1; 128.5; 129.0; 129.4; 129.8; 136.7; 141.0 (d, $J=7$ Hz); 176.0; high-resolution MS (CI+) calcd for $C_{15}H_{14}O_6P$: 321.0528, found 321.0542.

4-(Carboxy)phenylmethyl 4-(methoxy)phenylmethyl phosphate, dipotassium salt (18). The procedure described for **15** was followed using 4-methoxybenzyl alcohol instead of 4-nitrobenzyl alcohol. The resulting hapten was isolated as a white solid. ^1H NMR (250 MHz, CD_3CDOD) δ_H 3.74 (3H, s, $ArOCH_3$), 4.85 (4H, m, $ArCH_2$), 6.79 (2H, m, ArH), 7.29 (4H, m, ArH), 7.95 (2H, m, ArH); ^{13}C NMR (250 MHz, D_2O) δ_C 56.2; 67.7 (d, $J=6$ Hz); 68.2 (d, $J=6$ Hz); 114.7; 127.9; 128.3; 129.8 (d, $J=6$ Hz); 130.5; 136.1 (d, $J=6$ Hz); 140.9 (d, $J=6$ Hz); 159.2; 176.1; high-resolution FABMS calcd for $C_{16}H_{16}O_7P$: 351.0634, found 351.0670.

4-(Carboxy)phenylmethyl 4-(ethoxy)phenylmethyl phosphate, lithium salt, tetrabutylammonium salt (19). The procedure described for synthesizing haptens **5** and **6** was followed, using 4-ethoxybenzyl alcohol and methyl 4-(hydroxymethyl)benzoate as the two alcohols added to the 2-(trimethylsilyl)ethyl dichlorophosphite, yielding the product as a white solid. ^{13}C NMR (250 MHz, CD_3OD) δ_C 59.4, 64.4, 67.8 (d, $J=6$ Hz), 68.0 (d, $J=6$ Hz), 115.2, 127.5, 130.2, 130.4, 131.5, 138.2, 141.9, 160.0, 174.4; high-resolution FABMS calcd for $C_{17}H_{18}O_7P_1$: 365.0790, found 365.0816.

***N*-[2′-(Dimethylamino)ethyl] 4-(hydroxymethyl)benzamide.** 4-(Hydroxymethyl)benzoic acid pentafluorophenyl ester (8.0 g, 25.12 mmol) was dissolved in a minimal amount of dry dichloromethane. *N,N*-Diethylethylene diamine (2.516 g, 21.68 mmol) was added, and the mixture was stirred at room temperature for 48 h. The reaction mixture was washed with 5% aq NaOH and then with brine. The organics were dried over sodium sulfate, filtered

and concentrated in vacuo. The resultant brown oil was purified by flash chromatography (gradient elution with CH_2Cl_2:MeOH, 49:1→ CH_2Cl_2:MeOH, 9:1→ CH_2Cl_2:MeOH:triethylamine, 87:10:3) to provide the benzamide as a yellow oil. ^{1}H NMR (250 MHz, $CDCl_3$) δ_H 1.01 (6H, m, CH_2CH_3), 2.61 (6H, m, NCH_2), 3.45 (2H, m, $CONHCH_2$), 4.60 (2H, s, $ArCH_2OH$), 7.23 (2H, d, J=8 Hz, Ar*H*), 7.51 (1H, s, N*H*), 7.65 (2H, d, J=8 Hz, Ar*H*); ^{13}C NMR (250 MHz, $CDCl_3$) δ_C 11.0, 37.0, 46.9, 51.8, 63.9, 126.61, 127.1, 133.1, 144.8, 167.6; high-resolution MS (CI+) calculated for $C_{14}H_{23}N_2O_2$: 251.1760, found 251.17611.

4′-[*N*-2″-(Dimethylamino)ethyl]carbamoyl]phenylmethyl 4-nitrophenylmethyl carbonate (20). *N*-[2′-(Dimethylamino)ethyl] 4-(hydroxymethyl)benzamide (0.30 g, 1.2 mmol) and 4-nitrobenzyl chloroformate (0.31 g, 1.44 mmol) were dissolved in 1 mL pyridine and heated to 100 °C for 30 min. A white precipitate formed. The mixture was cooled to 50 °C and stirred for a further 12 h. During this time more 4-nitrobenzyl chloroformate (0.30 g) was added. The mixture was concentrated in vacuo, and the residue was purified via flash chromatography (gradient elution CH_2Cl_2:MeOH, 49:1→ CH_2Cl_2:MeOH, 23:2) to give the crude product as a brown oil. Further purification by chromatatron chromatography (gradient elution CH_2Cl_2→ $CHCl_2$:MeOH, 49:1→CH_2Cl_2:EtOH, 19:1) afforded the carbonate as a clear oil. ^{1}H NMR (250 MHz, CD_3CN) δ_H 1.22 (6H, m, CH_2CH_3), 3.03 (6H, m, NCH_2), 3.67 (2H, m, $CONHCH_2$), 5.19 (2H, s, $ArCH_2$), 5.25 (2H, s, $ArCH_2$), 7.43 (2H, d, J=8 Hz, Ar*H*), 7.56 (2H, d, J=8 Hz, Ar*H*), 7.99 (2H, d, J=8 Hz, Ar*H*), 8.17 (2H, d, J=8 Hz, Ar*H*), 8.64 (1H, broad s, CON*H*); ^{13}C NMR (250 MHz, CD_3CN) δ_C 9.6, 36.4, 48.4, 53.4, 68.9, 69.9, 124.6, 128.7, 128.8, 129.4, 135.3, 140.0, 144.1, 148.5, 155.6, 167.3; high-resolution MS (CI+) calcd for $C_{22}H_{28}N_3O_6$: 430.1978, found 430.1959.

4′-[*N*-2″-(Dimethylamino)ethyl]carbamoyl]phenylmethyl 4-nitrophenyl carbonate. *N*-[2′-(Dimethylamino)ethyl] 4-(hydroxymethyl)benzamide (0.990 g, 3.96 mmol) was dissolved in a minimal amount of dry dichloromethane. Pyridine (0.43 mL, 5.2 mmol) and 4-nitrophenyl chloroformate (1.04 g, 5.15 mmol) were added, and the reaction was stirred at room temperature for 24 h. The mixture was concentrated in vacuo and purified by flash chromatography (gradient elution with CH_2Cl_2:MeOH, 97:3→ CH_2Cl_2:MeOH, 22:3) to give the product as a white solid. ^{1}H NMR (250 MHz, $CDCl_3$) δ_H 1.42 (6H, m, CH_2CH_3), 3.21 (6H, m, NCH_2), 3.92 (2H, m, $CONHCH_2$), 5.31 (2H, s, $ArCH_2$), 7.40 (2H, m, Ar*H*), 7.50 (2H, d, J=8 Hz, Ar*H*), 8.15 (2H, d, J=8 Hz, Ar*H*), 8.28 (2H, m, Ar*H*).

4-Chlorophenylmethyl 4′-[*N*-2″-(dimethylamino)ethyl]-carbamoyl]phenylmethyl carbonate (21). 4-Chlorobenzyl chloroformate (0.142 g, 0.997 mmol) and NaH (0.024 g, 0.997 mmol) were dissolved in 45 mL dry THF and heated to 50 °C for 1 h. The solution was cooled and 4′-[*N*-2″-(dimethylamino)ethyl]carbamoyl]-phenylmethyl 4-nitrophenyl carbonate (0.20 g, 0.48 mmol) was added. The reaction was stirred at room temperature for 2 days. The cloudy orange mixture was vacuum filtered through a fritted glass funnel, and the yellow filtrate was concentrated in vacuo. Purification by flash chromatography (gradient elution CH_2Cl_2:EtOH, 49:1→ CH_2Cl_2:EtOH, 23:2) and chromatatron chromatography (CH_2Cl_2:EtOH, 49:1→CH_2Cl_2:EtOH, 23:2) afforded the carbonate as a yellow oil. ^{1}H NMR (250 MHz, CD_3CN) δ_H 1.03 (6H, m, CH_2CH_3), 2.63 (6H, m, NCH_2), 3.42 (2H, m, $CONHCH_2$), 5.12 (2H, s, $ArCH_2$), 5.18 (2H, s, $ArCH_2$), 7.39 (6H, m, Ar*H*), 7.79 (2H, m, Ar*H*); ^{13}C NMR (250 MHz, CD_3CN) δ_C 12.0, 38.1, 47.9, 52.7, 69.5, 69.7, 128.2, 128.8, 129.5, 130.8, 134.8, 135.5, 135.8, 139.9, 155.7, 167.2; high-resolution MS (CI+) calcd for $C_{22}H_{28}ClN_30_4$: 419.1738, found 419.1727.

4-[*N*-2′-(Dimethylamino)ethyl]carbamoyl]phenylmethyl phenymethyl carbonate (22). *N*-[2′-(Dimethylamino)-ethyl] 4-(hydroxymethyl)benzamide (0.2286 g, 0.913 mmol) and NaH (0.0219 g, 0.913 mmol) were dissolved in 45 mL dry THF and stirred at 45 °C for 1 h. The mixture was cooled to room temperature, and a solution of benzyl chloroformate (0.156 g, 0.913 mmol) in 10 mL dry THF was added via syringe. The reaction was stirred at room temperature for 36 h. The resulting cloudy orange solution was vacuum filtered through a fritted glass funnel, and the filtrate was concentrated in vacuo. Purification of the residue by flash chromatography (gradient elution CH_2Cl_2:MeOH, 99:1→ CH_2Cl_2:MeOH, 9:1) and chromatatron chromatography (CH_2Cl_2:MeOH, 49:1) afforded the carbonate as a clear oil. ^{1}H NMR (250 MHz, CD_3CN) δ_H 1.02 (6H, m, CH_2CH_3), 2.64 (6H, m, NCH_2), 3.44 (2H, m, $CONHCH_2$), 5.15 (2H, s, $ArCH_2$), 5.18 (2H, s, $ArCH_2$), 7.41 (7H, m, Ar*H*), 7.81 (2H, d, J=8 Hz, Ar*H*); ^{13}C NMR (250 MHz, CD_3CN) δ_C 11.9, 38.1, 47.9, 52.7, 68.6, 70.4, 118.3, 128.2, 128.8, 129.1, 129.4, 129.5, 135.7, 140.0, 155.8, 167.3; high-resolution MS (CI+) calcd for $C_{22}H_{29}N_2O_4$: 385.2127, found 385.2113.

4(-[*N*-2′-(Dimethylamino)ethyl]carbamoyl]phenylmethyl 4-methoxyphenylmethyl carbonate (23). *N*-[2′-(Dimethylamino)ethyl] 4-(hydroxymethyl)benzamide (0.161 g, 0.644 mmol) and NaH (0.0154 g, 0.644 mmol) were dissolved in 40 mL dry THF and stirred at 40 °C for 2 h. The cloudy yellow mixture was cooled to room temperature, and a solution of 4-methoxybenzyl *S*-(4,6-dimethylprimidin-2-yl)thiolcarbonate (0.098 g, 0.32 mmol) in 20 mL dry THF was added via syringe. The reaction was stirred at 35 °C for 5 h and then at room temperature for 3 days. Solvent was removed in vacuo, and the concentrate was purified via flash chromatography (gradient elution CH_2Cl_2:EtOH, 49:1→CH_2Cl_2:EtOH, 9:1) and chromatatron chromatography (gradient elution CH_2Cl_2:EtOH, 49:2→ CH_2Cl_2:EtOH, 23:2) to give the carbonate as a clear oil. ^{1}H NMR (250 MHz, CD_3CN) δ_H 1.01 (6H, m, CH_2CH_3), 2.59 (6H, m, NCH_2), 3.39 (2H, m, $CONHCH_2$), 3.77 (3H, s, OCH_3), 5.08 (2H, s, $ArCH_2$), 5.17 (2H, s, $ArCH_2$), 6.91 (2H, m, Ar*H*), 7.15 (1H, s, N*H*), 7.32 (2H, m, Ar*H*), 7.42 (2H, d, J=8 Hz, Ar*H*), 7.76 (2H, d, J=8 Hz, Ar*H*); ^{13}C NMR (250 MHz, CD_3CN) δ_C 12.3, 38.3, 47.8, 52.6, 55.9, 69.5, 70.3, 114.8, 128.1, 128.8, 131.2, 140.0, 155.8, 160.0, 160.9, 167.2, 176.6; high-resolution MS (CI+) calculated for $C_{23}H_{31}N_2O_5$: 415.2233, found 415.2219.

4-Ethoxyphenylmethyl 4′[*N*-2′-(Dimethylamino)ethyl]carbamoyl]-phenyl-methyl carbonate (24). 4-Ethoxybenzyl chloroformate (0.159 g, 1.05 mmol) and NaH (0.025 g, 1.05 mmol) were dissolved in 50 mL dry THF and heated to 50 °C for 1 h. The solution was cooled and 4′-[*N*-2″-(dimethylamino)ethyl]carbamoyl]-phenylmethyl 4-nitrophenyl carbonate (0.21 g, 0.505 mmol) was added. The mixture was stirred at room temperature for 6 days. The cloudy orange solution was vacuum filtered through a fritted glass funnel, and the filtrate was concentrated in vacuo. Purification by flash chromatography (gradient elution CH_2Cl_2:EtOH, 49:1→CH_2Cl_2:EtOH, 9:1) and chromatatron chromatography (gradient elution CH_2Cl_2:EtOH, 49:1→CH_2Cl_2:EtOH, 23:2) afforded the product carbonate. ^{1}H NMR (250 MHz, CD_3CN) δ_H 1.01 (6H, m, NCH_2CH_3), 1.34 (3H, m, OCH_2CH_3), 2.61 (6H, m, NCH_2), 3.40 (2H, m, $CONHCH_2$), 4.00 (2H, m, OCH_2CH_3), 5.07 (2H, s, $ArCH_2$), 5.16 (2H, s, $ArCH_2$), 6.88 (2H, d, J=8 Hz, Ar*H*), 7.29 (2H, m, Ar*H*), 7.42 (2H, d, J=8 Hz, Ar*H*), 7.78 (2H, m, Ar*H*); ^{13}C NMR (250 MHz, CD_3CN)$_C$ 12.2, 15.0, 38.3, 47.9, 52.6, 64.3, 69.5, 70.3, 115.3, 118.2, 128.1, 128.5, 128.8, 135.8, 140.0, 155.8, 160.2, 167.2; high-resolution MS (CI+) calcd for $C_{24}H_{33}N_2O_5$: 429.2389, found 429.2392.

Immunogen synthesis

1-Ethyl-3-(3-dimethylaminopropyl)carbodiimide (EDC) (6 mg, 0.032 mmol) and sulfo-NHS (4 mg, 0.019 mmol) were added to a solution of the hapten in 10 mM PBS. The concentration of the hapten varied with molecular weight to ensure approximately equal loading. After stirring for 10 min, a solution of 10 mg of keyhole limpet hemocyanin (KLH) in 10 mM PBS was added and the reaction allowed to stir for 1 h. After this time, the reaction mixture was diluted to 1 mg/mL protein with 10 mM PBS and dialyzed for 3 days into 10 mM PBS. After this time the immunogen was aliquoted, frozen, and stored at −20 °C. Another conjugate was prepared as described, substituting bovine serum albumin (BSA) for KLH. This conjugate was used for ELISA studies.

Rabbit immunizations and antibody purification

The immunogens prepared were used to immunize 5 lb, male New Zealand White rabbits (Diamond B Rabbitry, Stockdale, Texas), sets of 10 5-week old male BALB/cJ mice (Jackson Laboratories, Bar Harbour, Maine), or sets of 5-week old male outbred ICR mice (Harlan Sprague Dawley, Indianapolis, IN) according to published procedures[4,12,13] with immunizations every 21 days. The polyclonal antibody samples were isolated 10 days following immunization, and purified according to published procedures.[4]

Affinity constants by competition ELISA

Competition ELISA experiments were carried out according to standard procedures[13] using a 1 h at room temperature preincubation of antibodies with competitor on a separate plate, followed by a 10 min at room temperature incubation of this mix on an ELISA plate coated with the immunizing hapten–BSA conjugate. The absorbance values and their corresponding competitor concentrations were fed into a table using Kaleidagraph™ 3.0 and plotted using the following 1:1 binding curve equation to generate association constants:

$$A = \frac{A_o - (K_A\cdot[I] + K_A\cdot[Ab] + 1) - \sqrt{(K_A\cdot[I] + K_A\cdot[Ab] + 1)^2 - 4\cdot K_A\cdot[Ab]\cdot[I]}}{2\cdot K_A\cdot A_o/[Ab]}$$

where A_o = the maximal absorbance of uninhibited antibody, K_A = hapten:antibody equilibrium association constant, $[I]$ = concentration of competitor, and $[Ab]$ = concentration of antibody binding sites. The dissociation constants reported in the tables are calculated as $K_D = 1/K_A$.

$H_2{}^{18}O$ incorporation experiments

All $H_2{}^{18}O$ incorporation experiments were run with substrate **20** at a concentration of 125 μM in 1×Tris–HCl buffer (pH 8.0). Antibody, if used, was post-fifth injection rabbit anti-**15** antibody at 6.3 μM. $H_2{}^{18}O$ (95% $H_2{}^{18}O$, Fluka), when used, was 50% of the total reaction volume. Reactions were carried out in a dessicator at room temperature. Chemical ionization high resolution mass spectrometry was used to determine the relative amount of ^{18}O incorporation by comparing the heights of the peak at 430.2 mass units, the peak corresponding to substrate **20** with all O^{16}, and the peak at 432.2 mass units, corresponding to **20** containing one ^{18}O. The ratio of the two peak heights was compared to that obtained from substrate **20** samples allowed to hydrolyze in the absence of $H_2{}^{18}O$. Two different reaction times were used for each sample: 20 h, which is the time required for 10% of the substrate to be converted to product in the presence of the antibodies, and 66 h, the time required for 10% of the product to be converted to substrate in the absence of antibody.

Acknowledgments

We gratefully acknowledge financial support from the Searle Foundation (Chicago Community Trust), the Welch Foundation (#F-1188), and an NSF PYI award #CHE-9157440 to B.L.I.

References and Notes

1. Gallacher, G.; Jackson, C. S.; Searcey, M.; Badman, T.; Goel, R.; Topham, C. M.; Mellor, G. W.; Brocklehurst, K. *Biochem. J.* **1991**, *279*, 871–881.
2. Gallacher, G.; Searcey, M.; Jackson, C. S.; Brocklehurst, K. *Biochem. J.* **1992**, *284*, 675–680.
3. Gallacher, G.; Searcey, M.; Jackson, C. S.; Goel, R.; Mellor, G. W.; Brocklehurst, K. *Eur. J. Biochem.* **1993**, *214*, 197–207.
4. Stephens, D.; Iverson, B. L. *Biochem. Biophys. Res. Comm.* **1993**, *192*, 1439–1444.

5. Gallacher, G. *Biochem. Soc. Trans.* **1993**, *21*, 1087–1090.
6. Stephens, D. B.; Wilmore, B. H.; Iverson, B. L. *Bioorg. Med. Chem.* **1994**, *2*, 653–658.
7. Suzuki, H.; Sasaki, K.; Mukouyama, E.; Kawamura-Konishi, Y.; Wada, Y.; Ono, M. *Biochem. Mol. Biol. Int.* **1994**, *34*, 27–35.
8. Iverson, B. L. *CHEMTECH* **1995**, *25*, 17–21.
9. Shreder, K. R.; Thomas, R.; Wallace, M. B.; Helms, E.; Iverson, B. L. *Isr. J. Chem.* **1996**, *36*, 215–220.
10. Carter, S.; Resmini, M.; Simms, C.; Sreedharan, S. K.; Gallacher, G.; Brocklehurst, K. *Biochem. Soc. Trans.* **1997**, *25*, 86S.
11. Resmini, M.; Vigna, R.; Simms, C.; Barber, N.; Hagi-Pavli, E. P.; Watts, A. B.; Verma, C.; Gallacher, G.; Brocklehurst, K. *Biochem. J.* **1997**, *326*, 279–287.
12. Wilmore, B. H.; Iverson, B. L. *J. Am. Chem. Soc.* **1994**, *116*, 2181–2182.
13. Wallace, M. B.; Iverson, B. L. *J. Am. Chem. Soc.* **1996**, *118*, 251–252.
14. Basmadjian, G. P.; Singh, S.; Sastrodjojo, B.; Smith, B. T.; Avor, K. S.; Chang, F.; Mills, S. L.; Seale, T. W. *Chem. Pharm. Bull.* **1995**, *43*, 1902–1911.
15. Liu, D.; Yu, Y. *Ann. N. Y. Acad. Sci.* **1996**, *799*, 46–49.
16. Carter, S.; Resmini, M.; Simms, C.; Sreedharan, S. K.; Gallacher, G.; Brocklehurst, K. *Biochem. Soc. Trans.* **1997**, *25*, 86S.
17. Resmini, M.; Vigna, R.; Simms, C.; Barber, N. J.; Hagi-Pavli, E. P.; Watts, A. B.; Verma, C.; Gallacher, G.; Brocklehurst, K. *Biochem. J.* **1997**, *326*, 279–287.
18. Mu, Y. Q.; Gibbs, R. A. *Bioorg. Med. Chem.* **1997**, *5*, 1327–1337.
19. Pontoni, G.; Lopalco, L.; De Maria, S.; Zambardino, U.; Carteni Farina, M.; Siccardi, A. G.; Zappia, V. *Amino Acids (Vienna)* **1997**, *12*, 299–308.
20. Stephens, D. B.; Thomas, R. E.; Stanton, J. F.; Iverson, B. L. *Biochem. J.* **1998**, *332*, 127–134.
21. Resmini, M.; Gul, S.; Sonkaria, S.; Gallacher, G.; Brocklehurst, K. *Biochem. Soc. Trans.* **1998**, *26*, S170.
22. Butler, J. E. In *The Structure of Antigens*; Van Regenmortel, M. H., Ed.; CRC: Boca Raton, 1992; Vol. 1, pp 209–259.
23. Friguet, B.; Chaffotte, A. F.; Djavadi-Ohaniance, L.; Goldberg, M. E. *J. Immunol. Methods* **1985**, *77*, 305–319.
24. Underwood, A. P. *J. Immunol. Methods* **1993**, *164*, 119–130.
25. Prokipcak, J. M.; Breckles, T. H. *Can. J. Chem.* **1972**, *50*, 1770–1774.
26. Landsteiner, K. *The Specificity of Serological Reactions*, 2nd Ed.; Harvard University: Cambridge, 1945; pp 156–170.
27. Pauling, L.; Pressman, D.; Grossberg, A. L. *J. Am. Chem. Soc.* **1945**, *66*, 784–792.
28. Nisonoff, A.; Shaw, A. R.; Pressman, D. J. *J. Am. Chem. Soc.* **1959**, *81*, 1418–1423.
29. Linder, A. B.; Eshar, Z.; Tawfik, D. S. *J. Mol. Biol.* **1999**, *285*, 421–430.
30. Martin, S. F.; Josey, J. A. *Tetrahedron Lett.* **1988**, *29*, 3631–3634.
31. Mautz, D. S.; Davisson, V. J.; Poulter, C. D. *Tetrahedron Lett.* **1989**, *30*, 7333–7336.